
Proceedings Paper:
Zhang, G.B. and Li, G.-J. orcid.org/0000-0002-5956-4033 (2023) Comparative study of stator-mounted PM machines focusing on thermal performance. In: 2023 IEEE International Electric Machines & Drives Conference (IEMDC) Proceedings. 2023 IEEE International Electric Machines & Drives Conference (IEMDC), 15-18 May 2023, San Francisco, CA, United States. Institute of Electrical and Electronics Engineers (IEEE) . ISBN 9798350399004

https://doi.org/10.1109/IEMDC55163.2023.10238952

Comparative Study of Stator-mounted PM Machines Focusing on Thermal Performance

G. B. Zhang
Department of Electronic and Electrical Engineering, The University of Sheffield
Sheffield, United Kingdom
gzhang24@sheffield.ac.uk

G. J. Li
Department of Electronic and Electrical Engineering, The University of Sheffield
Sheffield, United Kingdom
g.li@sheffield.ac.uk

***Abstract*—Stator-mounted permanent magnet (PM) machine attracts more and more attention for its high-power density, robust structure and easy for cooling. This paper will provide a comparison focusing on thermal aspect amongst three typical stator-mounted permanent magnet machines, i.e., doubly salient PM machine, flux-reversal PM machine and flux-switching PM machine. To be more comprehensive, a surface mounted PM machine has also been used to compare against the stator-mounted PM machines. The investigated machines have been compared at a wide speed range from 400rpm to 3600rpm because the rotation speed has great impact on loss distribution and heat transfer in the airgap. The computational fluid dynamics (CFD) thermal models of these machines have been built using Ansys CFX software to compare their thermal performances. It is found that, compared to other two stator-mounted PM machines, the flux-switching PM machine, with the highest torque but also the highest losses, always has higher temperature rise (highest peak temperature). Meanwhile, since the windings and magnets are both located on the stator, the magnet temperature of stator-mounted PM machine is very close to their winding temperature.**

Keywords—CFD model, stator-mounted PM machine, thermal analysis

I. INTRODUCTION

In recent years, stator-mounted permanent magnet (PM) machines have attracted significant attention in both academia and industry. There are three typical topologies of stator-mounted PM machines, i.e., doubly salient PM (DSPM) machine, flux-reversal PM (FRPM) machine and flux-switching PM (FSPM) machine [1]. Since the magnets and the armature windings are both located on the stator, the stator-mounted PM machines are more advantageous in terms of magnet cooling compared to their rotor-mounted counterparts. This is because the heat generated in magnets can be dissipated from the stator to the housing directly rather than crossing through the airgap between the stator and the rotor, which often has low thermal conductivity. Thermal analysis has been deemed critical for PM machine design because elevated temperature can deteriorate machine performance. For example, it is commonly known that every 10K of temperature rise over the rated temperature would result in a reduction of insulation lifetime by half [2]. At the same time, high temperature could also lead to irreversible demagnetization of magnets, which reduces permanently the machine's torque performance [3].

In [4], an overview about thermal management of electrical machines was given. This includes loss calculation, material properties, thermal modelling methods and cooling techniques. To overcome some of the challenges in thermal modelling, such as contact resistance estimation, winding model simplification and convection coefficient calculation, useful methods or empirical equations are stated in [5-7]. However, most research papers focus on the thermal analysis of rotor-mounted PM machine since they are more widely used in industry. There are several papers investigating thermal modelling of stator-mounted PM machines but they are more or less limited to the FSPM machines [8-12], because they have much higher torque density than the other two typical stator-mounted PM machines [13]. As the thermal modelling of DSPM machine or FRPM machine has not attracted much attention, there is not yet well-documented research reporting a comprehensive comparison amongst the three types of stator-mounted PM machines focusing on the thermal aspect.

Therefore, the objective of this paper is to compare the thermal performance of the three stator-mounted PM machines. In addition, a surface mounted PM (SPM) machine will also be considered in this paper, as a typical reference to compare against the stator-mounted PM machines. Rotation speed, which corresponds to the fundamental frequency of the injected current, has significant influence on loss distribution and heat transfer of the airgap between the stator and rotor, so the investigated machines will be compared within a wide range of speed from 400 to 3600 rpm. Section II will introduce the design parameters of the three investigated machines and will also detail the calculated losses, which will be the heat source in thermal models. Section III will present the computational fluid dynamics (CFD) thermal models built in Ansys CFX, which will be used to predict the temperature distribution of the investigated machines at different speeds.

II. KEY FEATURES OF INVESTIGATED PM MACHINES AND THEIR LOSSES CALCULATIONS

A. Key Features of the Investigated PM Machines

The FSPM machines with 12 slots and 10 poles (12/10) have been regarded as the most popular design. The original design parameters of a FSPM machine are obtained from [14]. In order to have a fairer comparison, all the investigated machines should have the same overall size, airgap length and fundamental frequency. However, a 12/10 DSPM machine or a 12/20 SPM that have the same fundamental frequency as the 12/10 FSPM machine, cannot achieve adequate torque performance. As a compromise, a 12/8 DSPM machine and 12/10 SPM machine have been adopted for the comparison. Meanwhile, the global optimization is necessary to optimize the investigated machines. Multi-objective genetic algorism has been used in JMAG software to improve the torque performance, reduce losses and reduce magnet consumption [13]. The optimized machines are chosen to have very similar slot areas, so that their copper losses can be approximately considered as the same. The three stator-mounted PM machines together with the SPM machine, which have been optimized, are shown in Fig. 1, and the key design parameters are shown in Table I. It could be found that the FSPM machine does have much higher torque density comparing with the

other two stator-mounted PM machines, while the SPM machine produces a same level of torque with similar magnet usage as the FSPM machine.

Table I Key parameters of optimized stator-mounted PM machines

	12s/8p DSPM	12s/10p FRPM	12s/10p FSPM	12s/10p SPM
Outer radius (mm)	45			
Airgap length (mm)	0.5			
Stack length (mm)	25			
Housing length (mm)	60			
N° of turns per phase	72			
Rated RMS current (A)	10.6			
Split ratio	0.56	0.72	0.58	0.68
Slot area (mm^2)	1214	1196	1177	1215
PM volume (mm^3)	9200	4577	12900	13400

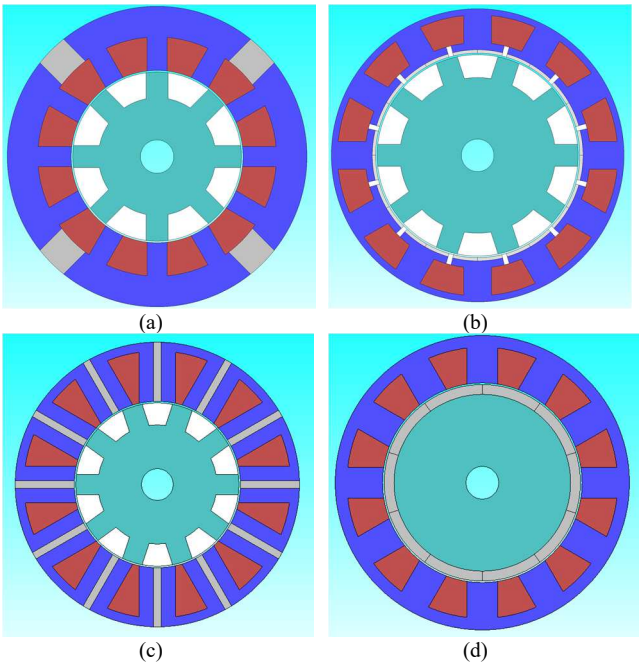

Fig. 1 Cross-sectional views of the optimized PM machines. (a) DSPM, (b) FRPM, (c) FSPM and (d) SPM machines.

B. Losses Calculations of the Investigated PM Machines

Losses including the copper losses in the windings, and the stator and rotor core losses as well as the PM eddy current loss, as the heat sources in the thermal modelling, play an important role in predicting temperature distribution. The copper loss (45W) in this paper is calculated by the rated phase rms current and the DC winding resistance, which will be maintained the same for all investigated machines. In order to simplify the comparison amongst the electrical machines, the temperature effect on losses (all losses have been calculated at 20°C) and the AC losses in the windings have not been considered. This simplification will not affect further comparison of these machines because they all have similar concentrated winding structure, meaning that their copper losses will be very much similar with or without considering those effects. In addition, the AC losses can be effectively restricted by using Litz wire. It has been tested in [15] that, the AC losses in winding could be only 2% more than the DC losses under 800Hz, while the highest frequency for the 12s/10p FSPM is only 600Hz. As for the PM eddy current loss, and the stator and rotor iron losses, they have all been obtained from 2D FEA simulation (JMAG software package).

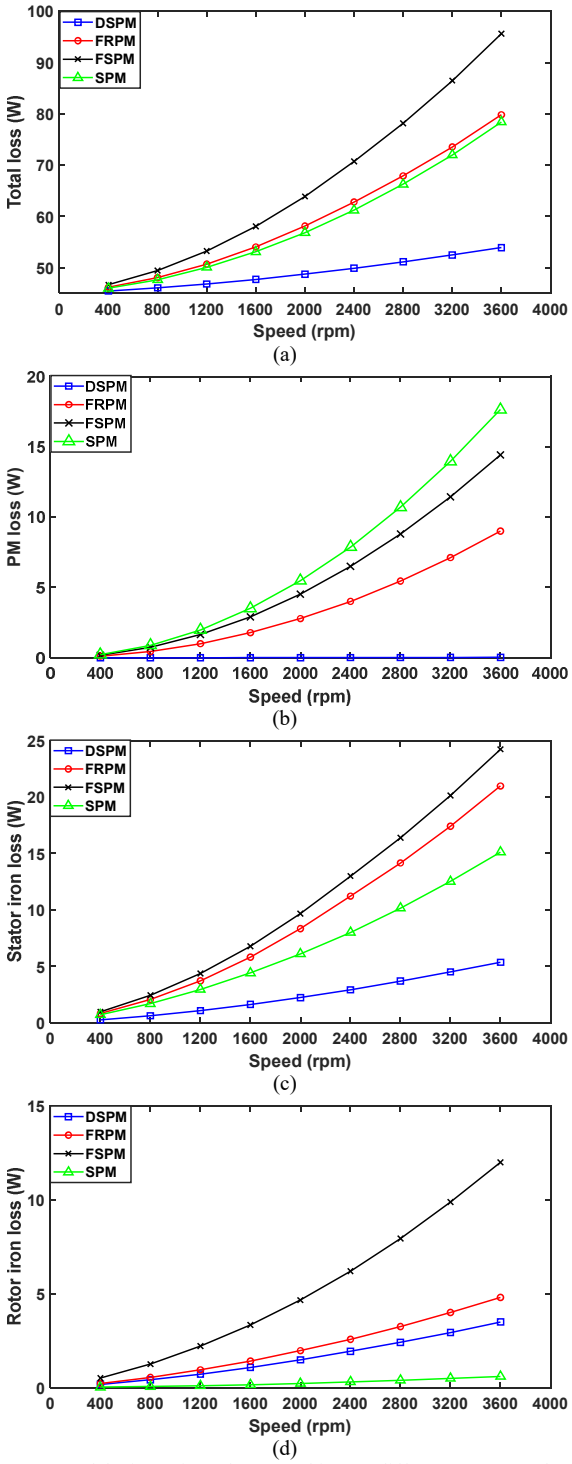

Fig. 2 Losses of the investigated PM machines at different rotor speeds (from 400rpm and 4000rpm). (a) Total loss, (b) PM eddy current loss, (c) stator iron losses, and (d) rotor iron losses.

Fig. 2 shows the loss distributions at a speed range between 400rpm and 3600rpm. It could be noticed that the FSPM machine has higher loss than the other machines especially at high speed range. As for the DSPM machine, with 20% lower fundamental frequency, it has the lowest total loss. And more importantly, the PM eddy current loss of the DSPM machine is negligible even at very high speed, which is very likely to lower the risk of magnet irreversible demagnetization. When it comes to the SPM machine, its total loss is still considerable and is close to the total loss of the FRPM machine, which has a similar magnetic circuit. It

should be noted that although the SPM machine has very small rotor iron loss, the SPM machine has the highest PM eddy current loss, which will be difficult to dissipate for a rotor-mounted PM machine.

III. CFD Thermal Modelling

The most popular methods for thermal modelling include lumped parameter thermal network (LPTN), finite element analysis (FEA) and computational fluid dynamics (CFD). CFD thermal model is usually considered to be the most accurate modelling method because the fluid flow characteristics can be predicted, while the LPTN and FEA models normally use empirical formulae to calculate heat transfer coefficients. As shown in Fig. 3, for stator-mounted PM machines with salient structure, the air flow in the airgap is often highly turbulent, and the existence of end region makes it more difficult to predict the air flow by empirical formulae [9]. Therefore, CFD models using Ansys CFX software have been built for the following investigations in this paper.

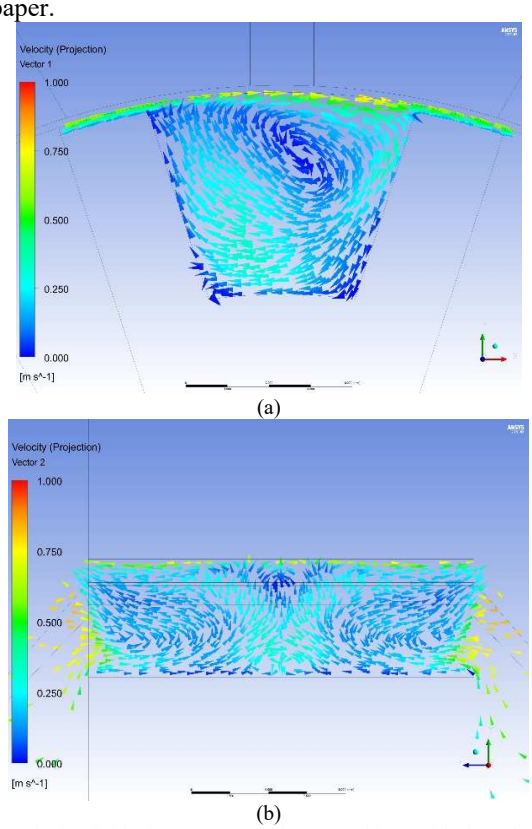

Fig. 3 Velocity field of stator mounted PM machines with the reference to the rotor at 400rpm. (a) radial direction, and (b) axial direction.

A. CFD Modelling of the Investigated PM Machines

The investigated machines have been built based on parameters listed in Table I. The CFD thermal models have considered all the solid zones of the investigated machines as well as air region including the airgap and the end space air region. In order to simplify the machine models and reduce the generated mesh numbers, only part of the machine stator and rotor are simulated according to their slot and pole number combination. The stationary region and rotation region of these machines are connected through pitch change connection, which is designed for sides that have unequal pitches in CFX. The turbulence model used in the simulation is shear stress transport (SST) turbulence model, which is an improved two-equation model developed in [16]. The rotation is modeled using frozen rotor model, meaning that the frame of reference is changed but the relative position of the components are maintained. In addition, in all simulations, it is assumed that air is an ideal gas with constant thermal parameters.

In the CFD thermal models, the essential thermal parameters of the solid components are listed in Table II, which are obtained from the material database of the Motor-CAD software package. Windings in the electrical machines are critical in the thermal analyses, because they are the important heat source and are composed of multiple layers of insulation and copper conductors. It would be very complicated to simulate the random wound coils in the CFD models. A popular solution is to represent the windings using equivalent thermal conductivity in different directions. Again, the equivalent thermal conductivities of the windings are obtained from the Motor-CAD software package, which are 0.87W/m^2·K in the circumferential and radial directions, and 265W/m^2·K in the axial direction.

Table II Essential thermal parameters of different machine materials

Component	Thermal Conductivity (W/m/°C)	Specific Heat (J/kg/°C)	Density (kg/m^3)
Housing	168	833	2790
Iron	30	460	7650
Coil	401	385	8933
Insulation	0.2	1700	1400
Magnet	7.6	460	7500
Shaft	52	460	7800

Apart from the winding model, some thermal contact resistances between the stator core and the housing are also essential to achieve an accurate temperature prediction. These thermal contact resistances are due to the imperfect contact between the surfaces and other factors like the material hardness, the interface pressure, the smoothness of the surfaces, and the air pressure will affect them significantly [5]. A useful method to represent the contact resistance is to use an equivalent airgap between the solid surfaces and the adopted airgap length is 0.03mm in this paper, the same as in [6]. In addition, the thermal model of the bearings is a complex problem, but it is also possible to solve this by using an equivalent interface gap. The adopted interface for bearings is 0.3mm in all simulations in this paper, again the same as in [6].

B. Natural Cooling of the Investigated PM Machines

The investigated PM machines are originally designed to be cooled down by natural cooling since the current density is only about 3.8A/mm^2 [4]. The convection coefficient of the housing surfaces is set to be 15W/m^2·K and the ambient temperature is 25°C. Because the winding insulation and PMs are the most vulnerable materials in the PM machines, the maximum temperatures of these components are monitored in Fig. 4. It can be seen that the three stator-mounted PM machines, all have slightly lower magnet temperature than their winding temperature, which can be regarded as a feature of the stator-mounted PM machine. This is because the magnets of the stator-mounted PM machines locate at the stator, which is close to the windings, hence the thermal resistance between the windings and the magnets is relatively

small especially compared to the thermal resistance of the airgap. As for the rotor-mounted PM machine, the magnet temperature would be lower than its winding temperature at low speed, but after a certain speed between 1200rpm and 2000rpm, the magnet temperature would be higher than the winding temperature and shows a rapid increasing trend. Temperature distributions at 400rpm and 3600rpm are chosen as examples to analyze these machines' thermal performance.

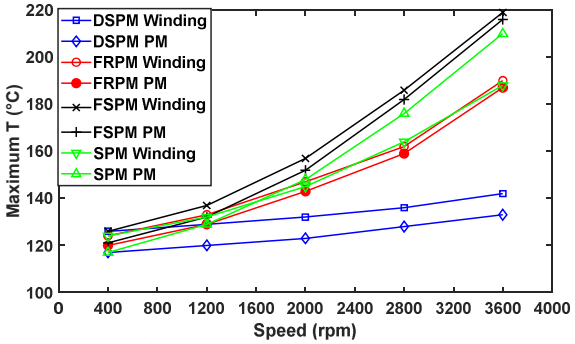

Fig. 4 Maximum winding temperature and maximum PM temperature.

The temperature distribution of the investigated machines at 400 rpm are shown in Fig. 5. When the rotor speed is 400 rpm, the overall temperature distributions of the four machines are quite similar. At this speed, the copper loss, which is maintained at 45W for all the machines, is the main heat source. However, it can still be seen that the winding temperatures of the FRPM machine and SPM machine are slightly lower than the other two machines at about 124°C. The FSPM machine has higher temperature mainly due to higher iron losses and PM eddy current loss, while for the DSPM machine, the thick back iron yoke and the position of the magnets increase the thermal resistance between the windings and the housing. But when it comes to the magnet temperature, the DSPM machine has the lowest magnet temperature of around 117°C. Compared with the FRPM and FSPM machines, it is found that the DSPM machine has superior magnet position, which is in the back iron, as the temperature difference between the windings and the magnets is rather large. The magnets in the stator back iron is so close to the housing that the heat generated inside them could be easily removed. It is worth mentioning that their low thermal conductivity could have a negative impact on the winding heat dissipation. Magnets of the FRPM machine are on the stator tooth surfaces adjacent to the airgap, so they are away from the stator housing (cooling system), which makes it rather difficult for the magnets in the FRPM machine to remove the heat. The magnet temperature of the FRPM machine is 120°C. The FSPM machine has a similar magnet temperature (121°C) as the FRPM machine, and it is also found that the temperature difference within the magnet of the FSPM machines is rather big, at around 8°C. This is because one end of the magnet is close to the airgap where the heat cannot be removed quickly, leading to higher temperature. However, the other end of the magnet is in contact with the housing where the heat can be easily removed, leading to lower temperature. As for the SPM machine, although the airgap successfully blocks the winding from heating the magnets, it is rather difficult for the magnets on the rotor to remove the heat. Therefore, the temperature of the SPM magnet is slightly higher than that of the DSPM machine but lower than those of the FSPM and FRPM machines.

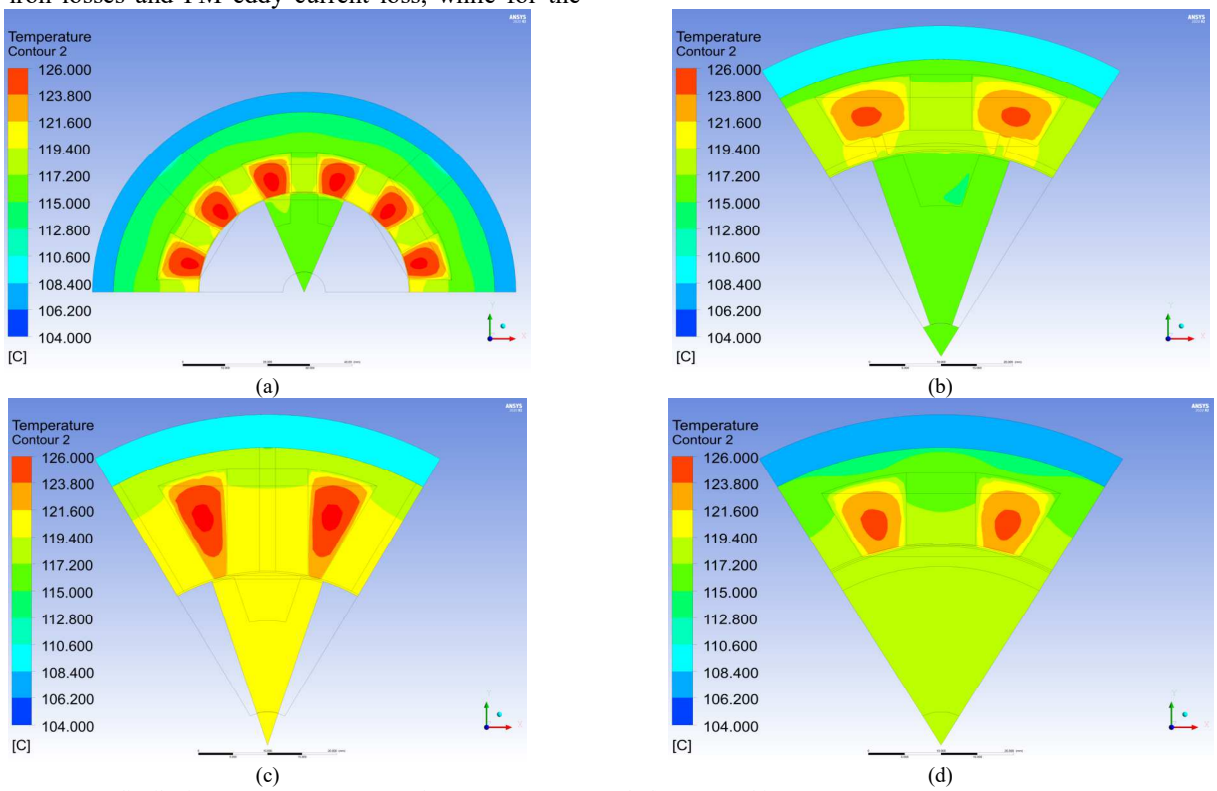

Fig. 5 Temperature distribution at 400rpm. (a) DSPM, (b) FRPM, (c) FSPM and (d) SPM machines.

As the rotor speed increases, iron losses and PM eddy current loss also increases rapidly as shown in Fig. 2, which will have a great impact on the temperature rise in the investigated machines. According to Fig. 4, both the winding temperatures and magnet temperatures show a rising trend as the rotor speed increases, but the temperature difference

amongst all these machines is big, as shown in Fig. 6. When the rotor rotates at 3600rpm, the DSPM machine, because it has the least total loss and negligible PM loss, also has lowest winding temperature and magnet temperature at 142°C and 133°C, respectively. As for the FRPM machine, with much lower iron losses and PM eddy current loss, the winding temperature is about 190°C and the magnet temperature is about 187°C. When it comes to the FSPM machine, its winding temperature can rise to 219°C and its magnet temperature can rise to 216°C, because it has significant PM eddy current loss and iron losses which are even higher than its copper loss. Another interesting finding about the FSPM machine at this speed is that the maximum temperature of the machine is not in the windings or magnets, it is located on the rotor. This is because at higher speed, the rotor iron loss increases more significantly. However, the airgap between the stator and rotor blocks the heat transfer route for the rotor, leading to increased rotor temperature. In the SPM machine, with huge PM eddy current loss, which is hard to dissipate due to the existence of airgap, it has a similar winding temperature as the FRPM machine at 188°C but a magnet temperature as the FSPM machine at 210°C.

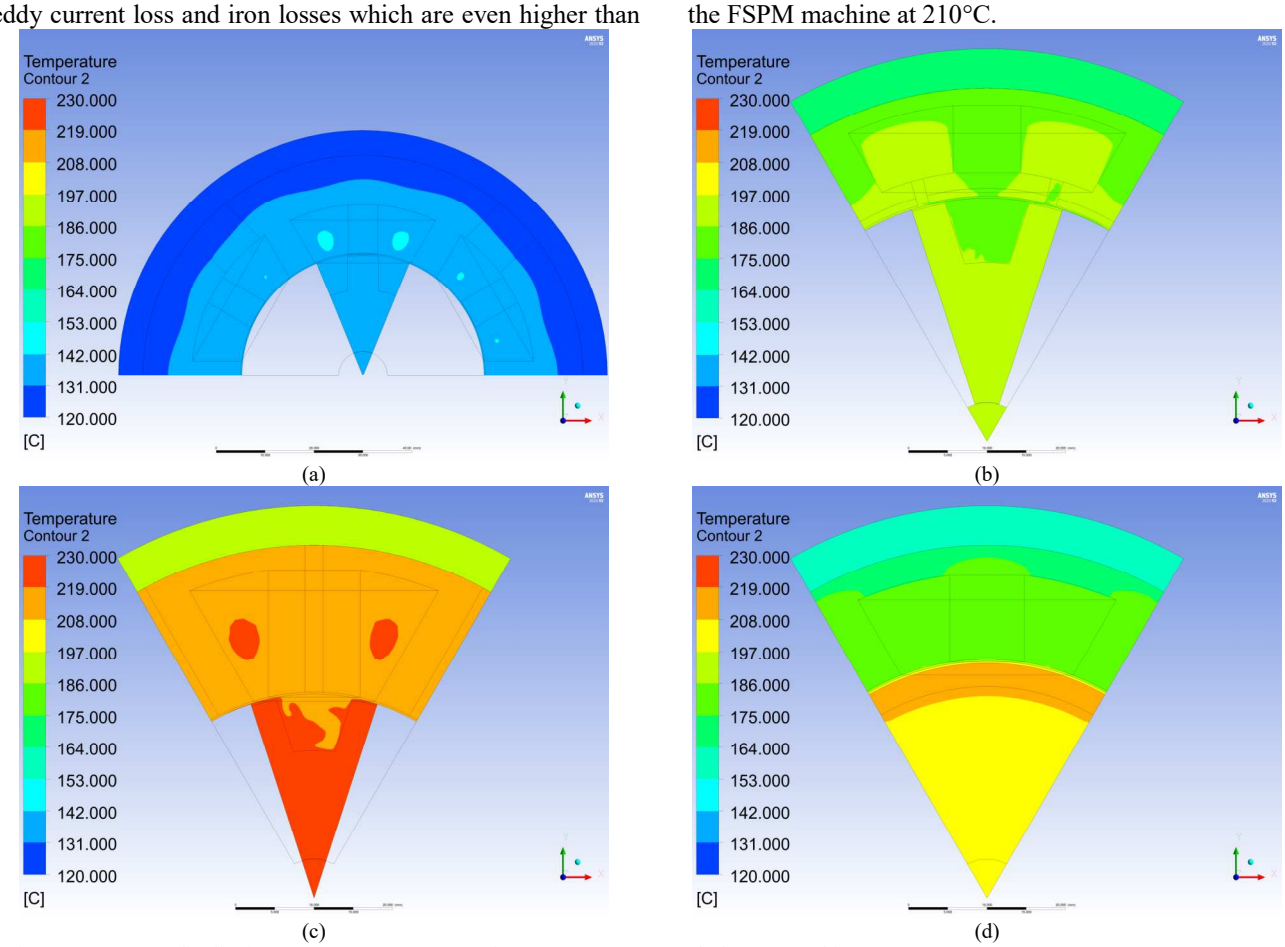

Fig. 6 Temperature distribution at 3600rpm. (a) DSPM, (b) FRPM, (c) FSPM and (d) SPM machines.

C. Water Jacket Cooling of the Investigated PM Machines

Fig. 6 shows that the winding and magnet temperature would be unreasonably high at 3600rpm, which clearly indicates that the natural cooling method is not sufficient in this case. In addition, it is also desirable to know whether the SPM and FSPM machines will have the same PM temperature with better stator cooling system. Therefore, the water jacket cooling has been employed when the rotor speed needs to be increased to 3600rpm or beyond. The geometry of the water jacket is shown in Fig. 7 (a). This water jacket consists of a spiral channel with three turns and its cross-sectional area is 40mm^2. In addition, the coolant inside the channels is water because it is low cost and has rather high thermal capacity. The water jacket is simulated in CFX software to derive the convective heat transfer coefficient (h_{water}) of the water jacket surface by (1) [9].

$$h_{water} = \frac{q_{wall}}{T_{wall} - T_{in}} \quad (1)$$

where q_{wall} is the heat flux that applied to the water jacket surface, T_{wall} represents average temperature of the water jacket surface and T_{in} is inlet temperature. Because the overall sizes of the investigated machines are rather small, the water jacket design is very conservative with a flow rate at only 0.6L/min. Assuming the inlet temperature is 25°C, the calculated heat transfer coefficient (h_{water}) is 779 W/m^2·K.

Fig. 8 shows the temperature distribution of the investigated PM machines operating at 3600rpm when the heat transfer coefficient of water jacket is applied on the machine housing. It could be noticed that even with a relatively conservative water jacket design, the windings and magnets have been effectively cooled down. The investigated machines all have a low winding temperature at around 50°C. Magnet temperatures of the three stator-mounted PM machines are still slightly lower than their winding

temperatures as it is explained in the previous section. However, the magnet temperature (77°C) of the SPM machine is significantly higher than the other stator-mounted PM machines. This indicates that the stator-mounted PM machines have better thermal performance than the rotor-mounted PM machines in high-speed application.

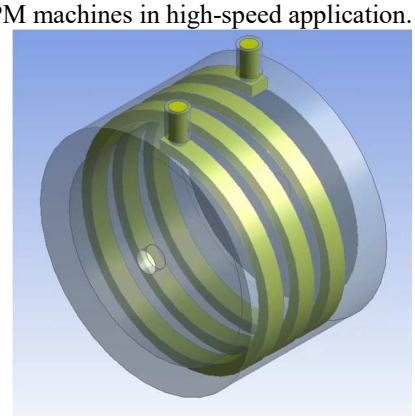

(a)

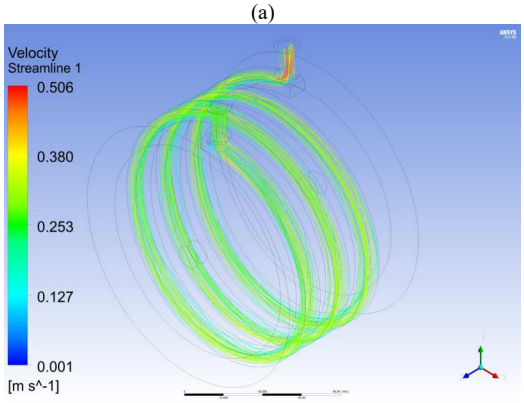

(b)

Fig. 7 Water jacket design. (a) Geometry, and (b) Velocity streamlines of water jacket.

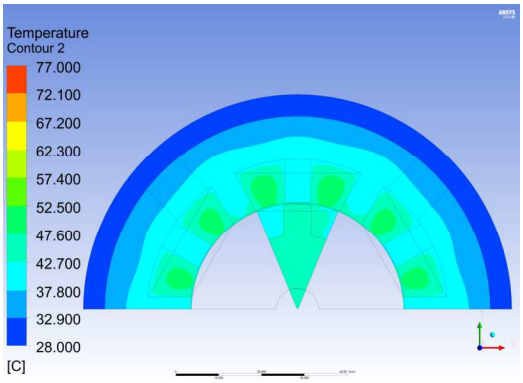

(a)

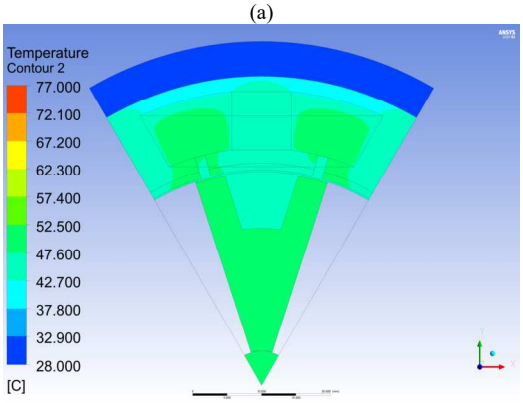

(b)

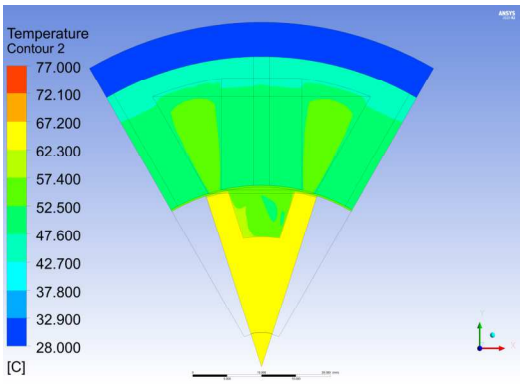

(c)

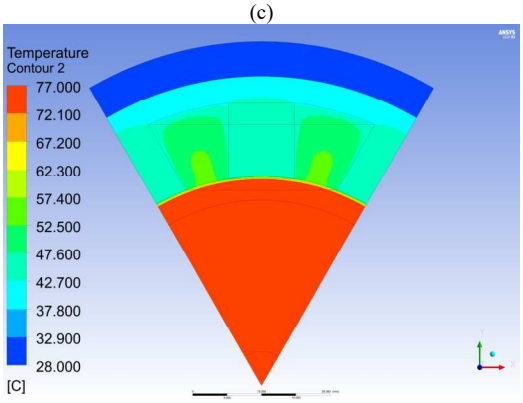

(d)

Fig. 8 Temperature distributions at 3600rpm. (a) DSPM, (b) FRPM, (c) FSPM and (d) SPM machines.

IV. Conclusion

This paper has compared the thermal performance of three typical stator-mounted PM machines and a SPM machine using CFD thermal modelling. In order to have a comprehensive comparison amongst these machines, a wide range of rotation speeds have been simulated and the corresponding PM eddy current losses and the stator and rotor core iron losses at different speeds have been calculated using 2D FEA. The investigated machines are designed to be cooled by natural air cooling or a rather conservative water jacket cooling if it is needed.

It is found that the FSPM machine, though it has the highest torque density, also generates much more iron losses and PM eddy current loss than the other two machines within a wide speed range. As a result, it often has much higher winding and magnet temperatures. As for the DSPM machine, it generates the least iron loss and negligible PM eddy current loss, hence its winding and magnet temperatures are always lower than the other machines. In addition, for stator-mounted PM machines whose winding and magnets are both located at the stator, their magnet temperature is very close to their winding temperature and they would change simultaneously. However, as for the SPM machine, the airgap will protect its magnets from overheating (by the windings) at low speed but also blocks heat removal when PM eddy current loss is large at high speed. Therefore, with an efficient cooling system like the water jacket, the stator-mounted PM machines will have better thermal performance than the rotor-mounted PM machines, especially for the magnets as they can achieve lower magnet temperature.

REFERENCES

[1] M. Cheng, W. Hua, J. Zhang, and W. Zhao, "Overview of stator-permanent magnet brushless machines," *IEEE Trans. Ind. Electron,* vol. 58, no. 11, pp. 5087-5101, 2011.

[2] E. L. Brancato, "Estimation of lifetime expectancies of motors," *IEEE Electr. Insul. Mag.,* vol. 8, no. 3, pp. 5-13, 1992.

[3] S. Zhu, M. Cheng, W. Hua, X. Cai, and M. Tong, "Finite element analysis of flux-switching PM machine considering oversaturation and irreversible demagnetization," *IEEE Trans. Magn.,* vol. 51, no. 11, pp. 1-4, 2015.

[4] Y. Yang, B. Bilgin, M. Kasprzak, S. Nalakath, H. Sadek, M.. Preindl, J. Cotton, N. Schofield and A. Emadi, "Thermal management of electric machines," *IET Electr. Syst. Transp.,* vol. 7, no. 2, pp. 104-116, 2017.

[5] D. Staton, A. Boglietti, and A. Cavagnino, "Solving the more difficult aspects of electric motor thermal analysis in small and medium size industrial induction motors," *IEEE Trans. Energy Convers.,* vol. 20, no. 3, pp. 620-628, 2005.

[6] A. Boglietti, A. Cavagnino, and D. Staton, "Determination of critical parameters in electrical machine thermal models," *IEEE Trans. Ind. Appl.,* vol. 44, no. 4, pp. 1150-1159, 2008.

[7] D. A. Staton and A. Cavagnino, "Convection heat transfer and flow calculations suitable for electric machines thermal models," *IEEE Trans. Ind. Electron.,* vol. 55, no. 10, pp. 3509-3516, 2008.

[8] G. Li, J. Ojeda, E. Hoang, M. Gabsi, and M. Lecrivain, "Thermal–electromagnetic analysis for driving cycles of embedded flux-switching permanent-magnet motors," *IEEE Trans. Veh. Technol.,* vol. 61, no. 1, pp. 140-151, 2011.

[9] M. Liu, W. Sixel, and B. Sarlioglu, "Comparative study of 6/4 FSPM and SPM machine for high-speed applications," in *2019 IEEE ITEC*, 2019, pp. 1-7: IEEE.

[10] Y. Hu, J. Wang, B. Li, B. Chen, M. Cheng, Y. Fan, W. Hua and Q. Wang, "Bidirectional coupling calculation of electromagnetic field and thermal field for FSPM machine," in *2020 IEEE ICIT*, 2020, pp. 139-144: IEEE.

[11] X. Cai, M. Cheng, S. Zhu, and J. Zhang, "Thermal modeling of flux-switching permanent-magnet machines considering anisotropic conductivity and thermal contact resistance," *IEEE Trans. Ind. Electron.,* vol. 63, no. 6, pp. 3355-3365, 2016.

[12] W. Yu, W. Hua, and Z. Zhang, "Cooling Analysis of High-Speed Stator-Permanent Magnet Flux-Switching Machines for Fuel-Cell Electric Vehicle Compressor," *IEEE Trans. Veh. Technol.,* vol. 71, no. 1, pp. 210-219, 2021.

[13] G. Zhang and G. Li, "Performance Comparison of Optimized Stator-Mounted Permanent Magnet Machines Focusing on PM Usage," in *2022 IEEE ECCE*, 2022, pp. 1-7: IEEE.

[14] Z. Zhu, Y. Pang, D. Howe, S. Iwasaki, R. Deodhar, and A. Pride, "Analysis of electromagnetic performance of flux-switching permanent-magnet machines by nonlinear adaptive lumped parameter magnetic circuit model," *IEEE Trans. Magn.,* vol. 41, no. 11, pp. 4277-4287, 2005.

[15] R. Wrobel, A. Griffo, and P. H. Mellor, "Scaling of AC copper loss in thermal modeling of electrical machines," in *2012 XXth ICEM*, 2012, pp. 1424-1429: IEEE.

[16] F. Menter, "Two-equation eddy-viscosity turbulence models for engineering applications," *AIAA journal,* vol. 32, no. 8, pp. 1598-1605, 1994.